An EEG Analysis Method Based on a Multivariate Scale Mixture Model and Related Application to Epileptic Seizure Detection

Ryota Onishi, Akira Furui, *Member, IEEE,* Akihito Takeuchi, Tomoyuki Akiyama, and Toshio Tsuji*, *Member, IEEE*

Abstract*—*Objective: **The detection of epileptic seizures in surface electroencephalogram (EEG) signals is an important problem in biomedical engineering. This paper proposes multichannel EEG analysis method based on a multivariate scale mixture model (SMM) that can be evaluated Gaussianity and non-Gaussianity by one dimensional parameter.** ***Methods:*** **In the model, a surface EEG signal at a certain time follows a multivariate Gaussian distribution, and its variance-covariance matrix is handled as a random variable that follows an inverse Wishart distribution. Thereby, we obtain by summing an infinite number of multivariate Gaussian distributions having different variance-covariance matrices. The proposed method combines a multivariate SMM with a filter bank, thereby allowing the time-series estimation of stochastic fluctuations latent in each frequency band of EEG. In addition, we introduce the index representing stochastic fluctuations based on the multivariate SMM parameter.** ***Results:*** **We applied the proposed method to the multichannel EEG data from twenty patients with focal epilepsy. The results demonstrated that the proposed index was significantly increased during epileptic seizures, especially in high frequency band. The index calculated in the high frequency band provided a higher classification performance between seizure segments and non-seizure segments (AUC = 0.881), which was significantly higher than the conventional amplitude-based index.** ***Conclusion:*** **This study proposed a multivariate scale mixture distribution-based stochastic EEG model capable of representing stochastic fluctuations associated with epileptic seizures. In high frequency band, proposed index shows the possibility of classification of epileptic seizures.** ***Significance:*** **The proposed model can be used in various fields of EEG, and helps to characterize stochastic fluctuations of multichannel EEG signals.**

***Index Terms*—Electroencephalogram (EEG), stochastic model, stochastic fluctuations, multivariate scale mixture model, epileptic seizures, non-Gaussianity.**

I. Introduction

EPILEPSY is a neurological disorder that causes epileptic seizures due to abnormalities in cranial nerves, and it is reported that there are around 50 million patients worldwide [1]. It is important to detect seizures early because leaving epileptic seizures can lead to increased brain damage. However, the diagnosis of epileptic seizures requires a lot of expertise and experience, and epileptic seizures can occur not only once but repeatedly [2]. Therefore, the diagnosis itself takes a long time, and the burden on doctors is a problem.

In order to reduce the burden on doctors, there have been many attempts to detect epileptic seizures using electroencephalogram (EEG), a bioelectric signal that can be recorded from the scalp [3]–[9]. For example, Deburachgrave *et al.* proposed EEG analysis focused on periodicity of high amplitude slow wave activity and sharp change in amplitude during seizures to detect epileptic seizures [3]. Subasi *et al.* also performed frequency analysis using wavelet transformation to identify epileptic seizures classification [4]. All the above methods, however, have a problem that it may be difficult to detect by evaluating only the magnitude of the amplitude or the change of the frequency because there are large individual differences in EEG during epileptic seizures due to age and type of epilepsy.

On the other hand, a study of the probability distribution shape of EEG has been conducted as a feature independent of amplitude and frequency [10]–[15]. It has long been common to assume that EEG signals followed a steady Gaussian distribution [10], [11], however, Campbell *et al.* statistically indicated that EEG signals had non-Gaussian properties [12], and so various analyzes focused on Gaussianity of EEG signals have been performed [11], [13]–[15]. Although there are few previous studies on the relationship between epileptic seizures and Gaussianity of EEG signals, Nurujjaman *et al.* and Charles *et al.* reported that EEG signals during epileptic seizures follows a non-Gaussian distribution [14], [15]. However, these studies are only experimental reports, and there is no theoretical framework to deal with non-Gaussianity of EEG signals quantitatively.

In this paper, we assume that non-Gaussianity of EEG signals is caused by stochastic fluctuations of amplitude, and propose an index that can estimate these fluctuations based on a multivariate scale mixture model (SMM). In the multivariate SMM, a surface EEG signal at a certain time recorded from multichannel electrodes follows multivariate Gaussian distribution, and its variance-covariance matrix is handled as a random variable that follows an inverse Wishart distribution. Thereby, it enables to evaluate the stochastic fluctuation of the variance-covariance matrix corresponding to the EEG amplitude. In addition, by combining this model with filter-bank, we develop an analysis method that can estimate stochastic fluctuations in each frequency band of EEG in a

R. Onishi, A. Furui and *T. Tsuji are with the Graduate School of Engineering,Hiroshima University, Higashi-hiroshima, 739-8527 Japan (e-mail: ryotaonishi@hiroshima-u.ac.jp; tsuji@bsys.hiroshima-u.ac.jp).

A. Takeuchi is with the Department of Neonatology, Okayama Medical Center, National Hospital Organaization.

T. Akiyama is with the Department of Child Neurology, Okayama University Hospital.

Manuscript received April 19, 2005; revised August 26, 2015.

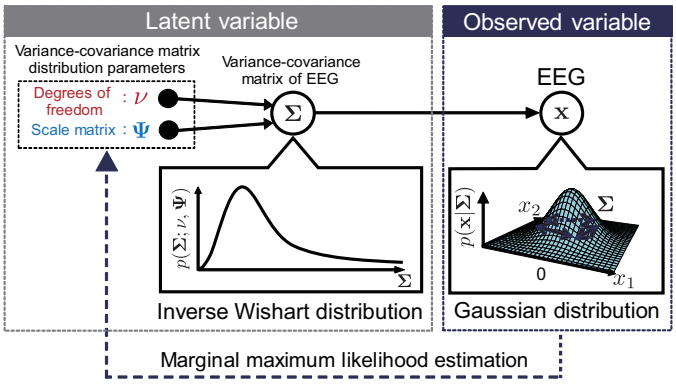

Fig. 1. Graphical representation of the stochastic relationship between EEG signals and its variance-covariance matrix. The white nodes are random variables and the black nodes are parameters to be estimated. In the model, EEG signals $\mathbf{x} \in \mathbb{R}^D$ are handled as a random variable that follows a multivariate Gaussian distribution with a mean vector of $\mathbf{0}$. The EEG variance-covariance matrix $\mathbf{\Sigma} \in \mathbb{R}^{D\times D}$ is also a random variable that follows the inverse Wishart distribution determined by the degrees of freedom parameter $\nu \in \mathbb{R}^+$ and the scale matrix $\mathbf{\Psi} \in \mathbb{R}^{D\times D}$. The parameter ν represents stochastic fluctuations of EEG signals. The variance-covariance matrix distribution parameters are estimated via marginal likelihood maximization from recorded EEG signals.

time series. In the simulation experiment, parameter estimation based on the proposed method is conducted on artificial data, and the error between the true value and the estimated value when the conditions are changed is discussed. In the analysis experiment, the analysis based on the proposed method was performed on the EEG signals during epileptic seizures. We verify the fitness of the proposed model and discuss the correspondence between the estimated stochastic fluctuations of EEG signals and the doctor's diagnosis.

The reminder of this paper is organized as follows: Section II outlines the structure of the multivariate SMM, the parameter estimation method, and EEG analysis method considering frequency charastalistic. Section III details the simulation experiments and epileptic EEG analysis experiments. Section IV presents the results of these experiments, and Section V provides related discussion. Finally, Section VI states the conclusions to this study.

II. Methods

A. Multivariate Scale Mixture Model of Surface EEG Signals

Fig. 1 shows the stochastic relationship between the EEG signals. In the proposed model, recorded EEG signals with D electrodes $\mathbf{x} \in \mathbb{R}^D$ and its variance-covariance matrix $\mathbf{\Sigma} \in \mathbb{R}^{D\times D}$ as a graphical model. $\mathbf{x}$ is handled as a random variable that follows a multivariate Gaussian distribution with a mean of zero and a variance-covariance matrix of $\mathbf{\Sigma}$. The variance-covariance matrix is also a random variable for which the distribution is determined by the degrees of freedom parameter $\nu \in \mathbb{R}^+$ and the scale matrix parameter $\mathbf{\Psi} \in \mathbb{R}^{D\times D}$.

First, the conditional distribution of EEG signals $\mathbf{x}$ given $\mathbf{\Sigma}$ is expressed via the following multivariate Gaussian distribution with mean of zero:

$$p(\mathbf{x}|\mathbf{\Sigma}) = \mathcal{N}(\mathbf{x}|\mathbf{\Sigma}) = \frac{1}{(2\pi)^{D/2}|\mathbf{\Sigma}|^{1/2}}\exp\left[-\frac{1}{2}\mathbf{x}^{\mathrm{T}}\mathbf{\Sigma}^{-1}\mathbf{x}\right]. \quad (1)$$

The distribution of the variance-covariance matrix is assumed to obey an inverse Wishart distribution $\mathcal{IW}(\mathbf{\Sigma};\nu,\mathbf{\Psi})$, which is known as a conjugate prior for the variance-covariance matrix of a multivariate Gaussian distribution:

$$p(\mathbf{\Sigma}) = \mathcal{IW}(\mathbf{\Sigma};\nu,\mathbf{\Psi}) = \frac{|\mathbf{\Psi}|^{\frac{\nu}{2}}}{2^{\frac{\nu D}{2}}\Gamma_D\left(\frac{\nu}{2}\right)}|\mathbf{\Sigma}|^{-\frac{\nu+D+1}{2}}\exp\left[-\frac{\mathrm{tr}(\mathbf{\Psi}\mathbf{\Sigma}^{-1})}{2}\right], \quad (2)$$

where ν and $\mathbf{\Psi}$ determine the inverse Wishart distribution, and are referred to as the degrees of freedom parameter and the scale matrix parameter, respectively. Considering the marginal distribution of $\mathbf{x}$, the variance-covariance matrix $\mathbf{\Sigma}$ can be integrated out as follows:

$$\begin{aligned} p(\mathbf{x}) &= \int p(\mathbf{\Sigma})p(\mathbf{x}|\mathbf{\Sigma})\mathrm{d}\mathbf{\Sigma} \\ &= \int \mathcal{IW}(\mathbf{\Sigma};\nu,\mathbf{\Psi})\mathcal{N}(\mathbf{x}|\mathbf{\Sigma})\mathrm{d}\mathbf{\Sigma} \quad (3) \\ &= \int \frac{|\mathbf{\Psi}|^{\frac{\nu}{2}}}{2^{\frac{\nu D}{2}}\Gamma_D\left(\frac{\nu}{2}\right)}|\mathbf{\Sigma}|^{-\frac{\nu+D+1}{2}}\exp\left[-\frac{\mathrm{tr}(\mathbf{\Psi}\mathbf{\Sigma}^{-1})}{2}\right] \\ &\quad \times \frac{1}{(2\pi)^{D/2}|\mathbf{\Sigma}|^{1/2}}\exp\left[-\frac{1}{2}\mathbf{x}^{\mathrm{T}}\mathbf{\Sigma}^{-1}\mathbf{x}\right]\mathrm{d}\mathbf{\Sigma} \\ &= \frac{|\mathbf{\Psi}|^{\frac{\nu}{2}}}{2^{\frac{\nu D}{2}}(2\pi)^{\frac{D}{2}}\Gamma_D\left(\frac{\nu}{2}\right)}\int |\mathbf{\Sigma}|^{-\frac{\nu+D+2}{2}} \\ &\quad \times \exp\left[-\frac{1}{2}\mathrm{tr}\{(\mathbf{\Psi}+\mathbf{x}\mathbf{x}^{\mathrm{T}})\mathbf{\Sigma}^{-1}\}\right]\mathrm{d}\mathbf{\Sigma} \\ &= \frac{\Gamma(\frac{\nu+1}{2})}{\Gamma(\frac{\nu-D+1}{2})}\frac{|\frac{1}{\nu-D+1}\mathbf{\Psi}|^{-\frac{1}{2}}}{[\pi(\nu-D+1)]^{\frac{D}{2}}}(1+\Delta)^{-\frac{\nu+1}{2}}, \quad (4) \end{aligned}$$

where Δ is the square of Mahalanobis' distance as follows:

$$\Delta = \mathbf{x}^{\mathrm{T}}\mathbf{\Psi}^{-1}\mathbf{x}. \quad (5)$$

From (1) and (3), $p(\mathbf{x})$ is obtained by summing an infinite number of multivariate Gaussian distributions having different variance-covariance matrices. As stated above, it can model marginal distribution of multidimensional EEG signals by Scale mixture distribution.

B. Parameter Estimation Based on Marginal Maximum Likelihood

Let us consider the estimation of ν and $\mathbf{\Psi}$, given N samples of EEG signals $\mathbf{X} = \{\mathbf{x}_n \in \mathbb{R}^D; n = 1, 2, \cdots, N\}$. The model parameters can be estimated by maximizing the marginal likelihood $p(\mathbf{X}) = \prod_{n=1}^{N} p(\mathbf{x}_n)$.

However, the maximum likelihood solution of marginal likelihood is generally complex, so it is difficult to optimize the solution analytically [16]. Therefore, we conduct this optimization of ν and $\mathbf{\Psi}$ based on the Expectation-maximization

(EM) algorithm [17] with the introduction of latent variable. To simplify (4), we defined the new parameters as:

$$\nu = \nu' + D - 1 \tag{6}$$

$$\mathbf{\Psi} = \nu'\mathbf{\Psi}'. \tag{7}$$

The marginal distribution can be expessed as

$$p(\mathbf{x}_n) = \int \mathcal{IW}(\mathbf{\Sigma}_n; \nu' + D - 1, \nu'\mathbf{\Psi}')\mathcal{N}(\mathbf{x}_n|\mathbf{\Sigma}_n)\mathrm{d}\mathbf{\Sigma}_n \tag{8}$$

$$= \frac{\Gamma(\frac{\nu'+D}{2})}{\Gamma(\frac{\nu'}{2})} \frac{|\mathbf{\Psi}'|^{-\frac{1}{2}}}{(\pi\nu')^{\frac{D}{2}}} \left(1 + \frac{\Delta'}{\nu'}\right)^{-\frac{\nu'+D}{2}}, \tag{9}$$

where

$$\Delta' = \mathbf{x}_n^{\mathrm{T}}(\mathbf{\Psi}')^{-1}\mathbf{x}_n. \tag{10}$$

Equation (9) is equivalent to multivariate Student-t distribution $\mathrm{St}(\mathbf{x}_n|\nu', \Psi')$ [16]. Accordingly, we redefine the latent variable and replace (8) with the following equivalent expression, thereby allowing the efficient calculation (refer to Appendix).

$$p(\mathbf{x}_n) = \int \mathrm{IG}(\tau_n; \nu'/2, \nu'/2)\mathcal{N}(\mathbf{x}_n|\tau_n\mathbf{\Psi}')\mathrm{d}\tau_n, \tag{11}$$

where τ_n is a new latent variable allowing inverse Gamma distribution $\mathrm{IG}(\cdot)$. The model parameters ν' and $\mathbf{\Psi}'$ are estimated by maximizing the marginal likelihood as outlined below.

(i) Initialize each parameter with the selection of arbitrary starting values.

(ii) *E-step*. Calculate the expectation of the complete-data log likelihood, denoted as $Q(\nu', \mathbf{\Psi}')$.

$$\begin{aligned} Q(\nu', \mathbf{\Psi}') &= \mathbb{E}\left[\ln \prod_{n=1}^{N} \mathrm{IG}(\tau_n; \nu'/2, \nu'/2)\mathcal{N}(\mathbf{x}_n|\tau_n\mathbf{\Psi}')\right] \\ &= \sum_{n=1}^{N}\Bigg[-\frac{D}{2}\ln(2\pi) - \frac{D}{2}\mathbb{E}[\ln\tau_n] - \frac{1}{2}\ln|\mathbf{\Psi}'| \\ &\quad - \frac{1}{2}\mathbb{E}\left[\tau_n^{-1}\right]\Delta' + \frac{\nu'}{2}\ln\frac{\nu'}{2} - \ln\Gamma\left(\frac{\nu'}{2}\right) \\ &\quad - \left(\frac{\nu'}{2} + 1\right)\mathbb{E}[\ln\tau_n] - \frac{\nu'}{2}\mathbb{E}\left[\tau_n^{-1}\right]\Bigg], \end{aligned} \tag{12}$$

where $\mathbb{E}\left[\tau_n^{-1}\right]$ and $\mathbb{E}[\ln\tau_n]$ are derived by calculating the posterior distribution $p(\tau_n|\mathbf{x}_n)$ of the latent variable τ_n as follows:

$$\mathbb{E}\left[\tau_n^{-1}\right] = \frac{\nu' + D}{\nu' + \Delta'}, \tag{13}$$

$$\mathbb{E}[\ln\tau_n] = -\ln\mathbb{E}\left[\tau_n^{-1}\right] + \ln\left(\frac{\nu'}{2}\right) - \psi\left(\frac{\nu'}{2}\right), \tag{14}$$

where $\psi(\cdot)$ is a digamma function.

(iii) *M-step*. Update the parameters by maximizing $Q(\nu', \mathbf{\Psi}')$. By setting the derivative of $Q(\nu', \mathbf{\Psi}')$ with $\mathbf{\Psi}'$ equal zero, the new scale matrix are obtained as

$${}^{\mathrm{new}}\mathbf{\Psi}' = \frac{1}{N}\sum_{n=1}^{N}\mathbb{E}\left[\tau_n^{-1}\right]\mathbf{x}_n\mathbf{x}_n^{\mathrm{T}}. \tag{15}$$

Because there is no closed form expression for the degrees of freedom parameter ν', we estimates ν' by maximazing $Q(\nu', \mathbf{\Psi}')$ based on a binary search.

$${}^{\mathrm{new}}\nu' = \arg\max_{\nu'} Q(\nu', {}^{\mathrm{new}}\mathbf{\Psi}'). \tag{16}$$

(iv) Evaluate the log-likelihood $\ln p(\mathbf{X})$ and repeat steps (ii)–(iv) until the calculation converges. Finally, estimated parameters ν' and $\mathbf{\Psi}'$ transform variance-covariance matrix distribution parameters ν and $\mathbf{\Psi}$.

Using this procedures, the parameters of the proposed model can be estimated from recorded EEG signals. Inverse Wishart distribution parameter ν corresponds to the degrees of freedom of multivariate Student-t distribution parameter, hence ν is a distribution parameter to determine Gaussianity. In the framework of the multivariate SMM, we consider Gaussianity changes because of stochastic fluctuations of parameter equivalent to variances. From the above, it can be evaluated fluctuations of variance-covariance matrix by estimating ν from recorded EEG signals.

C. Proposed EEG Analysis Methods

Figure 2 shows an overall outline of proposed analysis method. In proposed method, observed EEG signals were decomposed into multiple frequency bands by using filterbank consisting of parallel band-pass filters. Additionally, we estimate stochastic fluctuations for signals in each frequency band based on the multivariate SMM.

First, EEG signal at time t recorded from the D pair of electrodes is $\mathbf{x}_t \in \mathbb{R}^D$. Then, $\mathbf{x}_t$ is divided into M frequency bands $b_1, \cdots, b_M$ by applying a filter-bank consisting of a third-order Butterworth bandpass filter to the signal, and the obtained signal is defined as $x_t^{(b_m)}$ $(m = 1, \cdots, M)$. Second, parameter estimation of the variance-covariance matrix distribution based on the multivariate SMM is performed on $\mathbf{x}_t^{(b_m)}$ for each frequency band, and ν characterizing the stochastic fluctuation is obtained. Here, a sliding window length W (s) is applied to the signal $\mathbf{x}_t^{(b_m)}$ in each band, and parameter ν are estimated based on the procedure of II–*B* for the sample in the window, since characteristics of EEG signals change greatly in a time series. By estimating this sliding window with a sliding width S (s) continuously, it is possible to obtain the estimation results of ν in time series. Here, ν is a parameter that means that the closer to ∞, the closer the distribution approaches a Gaussian distribution, that is, the smaller the stochastic fluctuation. In this paper, we calculate $1/\nu$, that is the reciprocal of ν, and use it as an index to characterize the stochastic fluctuation. The value of $1/\nu$ indicates that the larger the value, the larger the stochastic fluctuation of the EEG signal.

From the above, stochastic fluctuations implicit in each band of EEG signals can be acquired in time series. It is also possible to obtain the spatial distribution of stochastic fluctuations by dividing the EEG electrode arrangement into multiple regions in advance and performing the above analysis for each region.

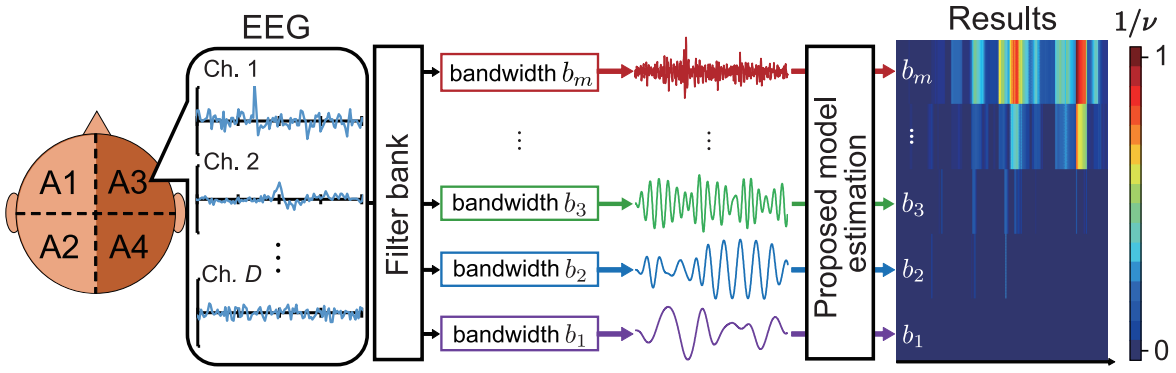

Fig. 2. Overview of the proposed analysis method. The recorded EEG signals are decomposed into b_1–b_m frequency band by using filterbank consisting of parallel band pass filters, then the parameter is estimated based on the proposed model and show the results by using color map.

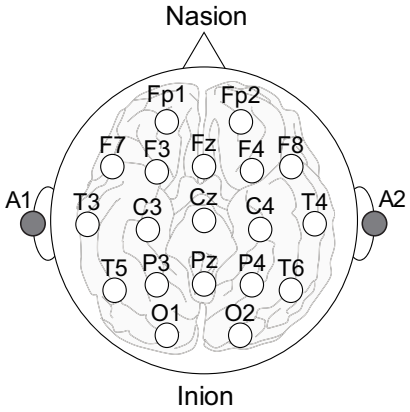

Fig. 3. International 10–20 electrode montage

III. Experiments

A. Simulation

To verify the accuracy of estimation based on the multivariate SMM, we performed a simulation experiment to evaluate the error rate between the estimated value and the measured value. Using the fact that the marginal distribution of the proposed model is equivalent to the multivariate t-distribution, a random number sequence $\{\mathbf{x}_t \in \mathbb{R}^D(t = 1, \cdots, T)\}$ following multivariate t-distribution $\mathrm{St}(\mathbf{x}_t|\nu_0', \mathbf{\Psi}_0')$ was generated. Here, the $\{\mathbf{x}_t\}$ values were regarded as a time series of an EEG signal recorded at the sampling frequency of f_s. The accuracy of distribution estimation was verified by comparing true values ν_0 and $\mathbf{\Psi}_0$ with estimate values ν and $\mathbf{\Psi}$, after converting ν_0' and $\mathbf{\Psi}_0'$ to inverse Wishart distribution parameters based on is (6) and (7). As an index of estimation accuracy for each parameter, the absolute percentage error was defined as $|\nu_0 - \nu|/|\nu_0| \times 100$, $\|\mathbf{\Psi}_0 - \mathbf{\Psi}\|_F/\|\mathbf{\Psi}_0\|_F \times 100$, where, $\|\mathbf{\Psi}\|_F$ is the Frobenius norm of $\mathbf{\Psi}$ [18], and using the element ψ_{ij} of $\mathbf{\Psi}$, it is obtained as follows:

$$\|\mathbf{\Psi}\|_F = \sqrt{\sum_{i=1}^{D}\sum_{j=1}^{D}|\psi_{ij}|^2}. \tag{17}$$

In the estimation of each parameter, the first W values of the signals $\{\mathbf{x}_t\}$ were used. The window length W took values of 1, 2, 5, 10, 15, 20, 30, 50, 100 s, and the number of dimensions D took values of 1, 2, 4, 8, 16, 19. The average absolute percentage errors were calculated by changing the true values of multivariate t-distribution parameters: the degrees of freedom ν_0' and the scale matrix $\mathbf{\Psi}_0'$ 400 times ($\nu_0' = 0.5, 1.0, 1.5, \cdots, 10.0, \psi_{0ii}' = 1.0, 2.0, 3.0, \cdots, 20.0$). Note that $\mathbf{\Psi}_0'$ is changed only for the diagonal components ψ_{0ii}', and the off-diagonal components were fixed at 0.5. The T and f_s values in artificial data were set as 100 s and 500 Hz.

B. Epileptic EEG analysis

In this experiment, we evaluated the validity of the proposed model and verify the validity the effectiveness of the proposed index$1/\nu$. The subjects were 20 epileptic patients with focal epilepsy, and EEG signals recorded in the supine position. Table I shows the information of each subject, analysis time, and duration of epileptic seizures. The EEG was recorded with a digital sampling frequency at 500 Hz by using EEG instrument (Neurofax EEG-1218, Nihon Kohden, Tokyo, Japan). Surface electrodes ($D = 19$) placed on the scalp according to the international 10–20 electrode system with reference electrodes on both earlobes: A1, A2 (refer to Fig. 3). The analysis in this paper was performed with the approval by the Okayama University Ethics Committee.

For all EEG signals of all subjects, we performed the fitting of the proposed model and calculated the index $1/\nu$ based on II.C. We set the frequency bands to $b_m \in \{\delta, \theta, \alpha, \beta, \gamma\}$, and decomposed EEG signals into δ (1–3 Hz), θ (4–7 Hz), α (8–12 Hz), β (13–24 Hz), γ (25–100 Hz). These frequency bands are generally used to extract features of EEG signals [19]. Here, fitting of the model and calculation of $1/\nu$ were performed continuously using a sliding window with window length W = 15 s and sliding width S = 1 s.

First, we performed to verify the validity of the proposed model for EEG signals in each frequency band. As an evaluation index of fitness, BIC (Bayesian information criterion) [20] that balances the model's fitness and complexity was used.

TABLE I
SUBJECT CONDITIONS

Subject	Sex	Age (year)	Total data length (s)	Seizure duration (s)
Sub. A	Male	2	300	71
Sub. B	Male	23	300	54
Sub. C	Male	2	300	71
Sub. D	Male	4	380	93
Sub. E	Female	31	320	39
Sub. F	Male	41	300	32
Sub. G	Female	3	240	53
Sub. H	Male	19	390	36
Sub. I	Male	0.8	360	98
Sub. J	Male	20	390	16
Sub. K	Male	36	300	23
Sub. L	Male	9	300	43
Sub. M	Male	13	300	43
Sub. N	Male	15	300	48
Sub. O	Male	8	300	17
Sub. P	Female	19	300	69
Sub. Q	Male	27	420	62
Sub. R	Male	38	300	65
Sub. S	Male	17	300	17
Sub. T	Male	19	300	65

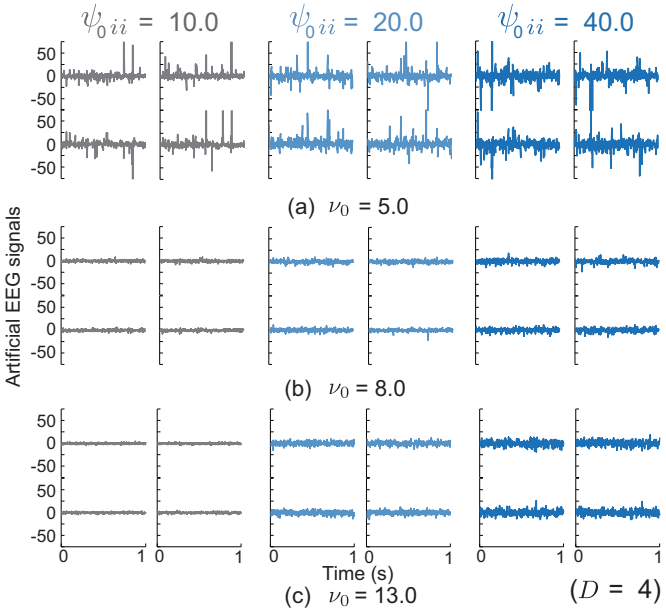

Fig. 4. Examples of artificially generalized EEG signals (D = 4) with ν_0 set to (a) $\nu_0 = 5.0$, (b) $\nu_0 = 8.0$, and (c) $\nu_0 = 13.0$; in each case, ψ_{0ii} was set to $\psi_{0ii} = 10.0$, $\psi_{0ii} = 20.0$, and $\psi_{0ii} = 40.0$.

$$\mathrm{BIC} = -2\ln L(\hat{\theta}) + k\ln(N_W), \tag{18}$$

where, $\ln L(\hat{\theta})$ is the likelihood of the model, k is the number of parameters estimated by models, and N_W is the sample size in the sliding window. BIC was calculated for the fitting results for each sliding window. For comparison, BIC was also calculated for the multivariate Gaussian model and the multivariate Cauchy model with a heavy tail.

Second, to verify the effectiveness of the evaluation of EEG stochastic fluctuations based on the proposed method, we evaluated the classification performance of epileptic and non-epileptic seizures by using the calculated indices $1/\nu$ of each frequency band (δ–γ band). The calculated results of $1/\nu$ for each subject were divided into those obtained from the seizure interval and those obtained from the non-seizure interval. Here, the non-seizure interval is defined as the period from the start of the analysis to the onset of seizures, and the interval in which the effects of noise due to body motion or electrode shift in the original EEG signals were remarkably excluded. In addition, since the sample size of $1/\nu$ differs greatly between the seizure and non-seizure intervals, the sample size of the non-seizure interval is extracted based on the sample size of the seizure interval, and the sample size of $1/\nu$ was adjusted for each subject.

As an evaluation of classification performance, We calculated area under curve (AUC) based on receiver operating characteristic analysis (ROC). AUC is an evaluation scale calculated from the ROC curve plotting the relationship between the false positive rate and the true positive rate. The closer the value is to 1, the higher the classification performance. For comparison, AUC was calculated in the same way using only the EEG amplitude information. The root mean square (RMS) [21] was used for the amplitude information as follows:

TABLE II
PERCENTAGE OF THE TIMES EACH MODEL WAS SELECTED FOR DIFFERENT FREQUENCY BANDS.

Frequency band	BIC		
	Proposed	Gaussian	Cauchy
δ	81.80%	17.92% *	0.28% *
θ	95.47%	4.42% *	0.11% *
α	96.79%	3.09% *	0.12% *
β	99.05%	0.59% *	0.36% *
γ	99.28%	0.21% *	0.51% *

*: Comparisons between proposed model and the others based on the McNemar test with a Holm adjustment ($p < 0.001$).

$$\mathrm{RMS} = \sqrt{\frac{1}{N_W}\sum_{i=1}^{N_W}(x_i^{\mathrm{Cz}})^2}, \tag{19}$$

where, x_i^{Cz} is EEG signal at Cz obtained from the top of the head. This RMS was calculated continuously using a sliding window with the same settings as when calculating $1/\nu$.

IV. RESULTS

A. Simulation

Fig. 4 shows an example of time-series waveforms with the parameters of inverse Wishart distribution in artificial data generation as $\nu_0 = \{5.0, 8.0, 13.0\}$, $\psi_{0ii} = \{10.0, 20.0, 40.0\}$. The vertical and horizontal axes indicate the signal values and time, respectively.

Fig. 5 shows the average absolute percentage error of the estimated ν and $\mathbf{\Psi}$ by changing the window length W and the number of dimensions D.

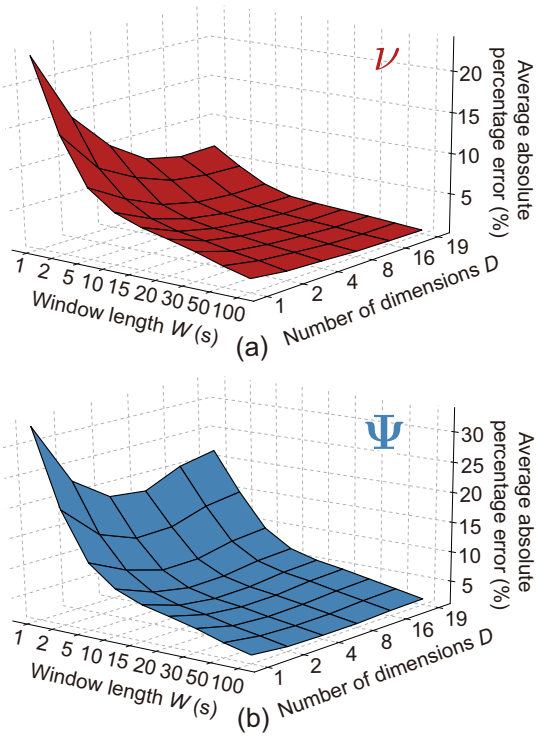

Fig. 5. Average absolute percentage errors for each combination of the number of input dimensions D and the length of the sliding window W in the estimation of variance-covariance distribution parameters. (a) ν. (b) $\mathbf{\Psi}$.

B. Epileptic EEG analysis

Table II shows percentage of the times that BIC of each model became minimum in EEG signals of δ–γ band. The table also shows the results of the McNemar test (significance level: 1%) adjusted by the Holm method using the proposed model as a control group. Fig. 6 shows the calculation results of $1/\nu$ corresponding to the raw EEG waveforms in Sub. A and Sub. B by a color map. In this color map, $1/\nu$ was normalized so that the maximum value of all frequency bands is 1 and the minimum value is 0. The shaded area in the waveforms and the white dotted line in the color map were sections that a doctor diagnosed an epileptic seizure.

Fig. 7 shows the distribution of $1/\nu$ in each frequency band for all subjects calculated by kernel density estimation [22] for each seizure and non-seizure interval. In the figure, the results of the paired t test (significance level: 1%) and the effect size g [23] are also shown. Here, the effect size g is a statistical index indicating the magnitude of the difference between the mean values of the two distributions. Generally, $0.2 \leq g < 0.5$ is interpreted as a small effect size, and $0.5 \leq g < 0.8$ is a medium effect size, $0.8 \leq g$ is a large effect size [24].

Fig. 8(a) shows the ROC curves obtained by seizure and non-seizure classification for each of $1/\nu$ in each frequency band and RMS as amplitude information. The AUC obtained from the ROC curve are also shown in Fig. 8(b). The AUC of $1/\nu$ in each frequency band (δ–γ) was 0.709, 0.647, 0.615, 0.727, 0.881, respectively, and the AUC of RMS was 0.816. The results of the test of the area under the curve [25] adjusted by the Holm method using the conventional feature, RMS as a control group are also presented (significance level: 1%).

V. Discussion

In the simulation experiment, as the value of ν_0 changes from $\nu_0 = 5.0$ to $\nu_0 = 13.0$, it can be seen that outliners of the waveform don't appear frequently and the waveform is steady. This indicates that the distribution approaches the Gaussian distribution as the value increase because ν is a parameter that determines the Gaussianity of the distribution. In the value of ψ_{0ii}, it can also be seen that the amplitude of the artificial data increases as the value of ψ_{0ii} changes from $\psi_{0ii} = 10.0$ to $\psi_{0ii} = 40.0$. This is because ψ_{ii}, that the diagonal component of $\mathbf{\Psi}$, is a parameter that characterizes the variance scale of EEG signals in each dimension.

In Fig. 5, the average absolute percentage error of ν and $\mathbf{\Psi}$ is about 2 % at W = 100 s, indicating the estimation is accurate. The error rate, however, increases up to about 25% in ν, and about 35% in $\mathbf{\Psi}$ at respectively W = 1 s, when the window length W is decreased. This results indicate that the accuracy depends on the window length. When the number of dimensions D was increased, the average absolute percentage error of ν also decreased, and that of $\mathbf{\Psi}$ decreased once and increased again. ν is a parameter defined as one dimension for the entire input dimension, therefore, it is considered that increasing the number of dimensions increased the actual sample size to be estimated, and decreased the average absolute percentage error. $\mathbf{\Psi}$ is affected by the estimation accuracy of ν' from $\mathbf{\Psi} = \nu'\mathbf{\Psi}'$, therefore, the error rate is considered to increase synergistically when the number of dimensions decreased. On the other hand, it can be seen the average absolute percentage error of $\mathbf{\Psi}$ increased when the number of dimensions increased. It is considered that the average absolute percentage error increased because the calculation was performed using the Frobenius norm even though the number of elements in the matrix increased and the estimation accuracy for each element did not change.

From the above, as the window length is increased, the estimation of ν and $\mathbf{\Psi}$ is perfomred more accurately, and as the number of dimensions is increased, the estimation of ν is perfomred more accurately. By contrast, the estimation accuracy of $\mathbf{\Psi}$ is decreased. These results indicate that in 19 dimension with international 10–20 electrode montage, when the window length is larger than 5 s, it can be estimated with an error rate at least 10% or less, especially when W = 15 s, with an error rate about 5%. 以上のことから，窓幅を大きくすることで，ν，$\mathbf{\Psi}$ はより正確に推定を行なうことができ，次元数を大きくすることで ν はより正確に，反対に $\mathbf{\Psi}$ の推定精度は減少することがわかった．これらの結果より，international 10–20 electrode system で用いられる電極数である 19 次元において，窓幅が 5 s 以上であれば，少なくとも 10%以下の誤差, 特に W = 15 s の場合は 5%程度の誤差で推定が行なえると考えられる．

In the EEG analysis experiment, it can be seen that BIC of proposed model has the smallest number of times in each frequency band (Table II). 脳波解析実験において，Table II より，各周波数帯域において，提案モデルの BIC が最も最小となる回数が多いことがわかる．しかし，δ 帯域の場合，

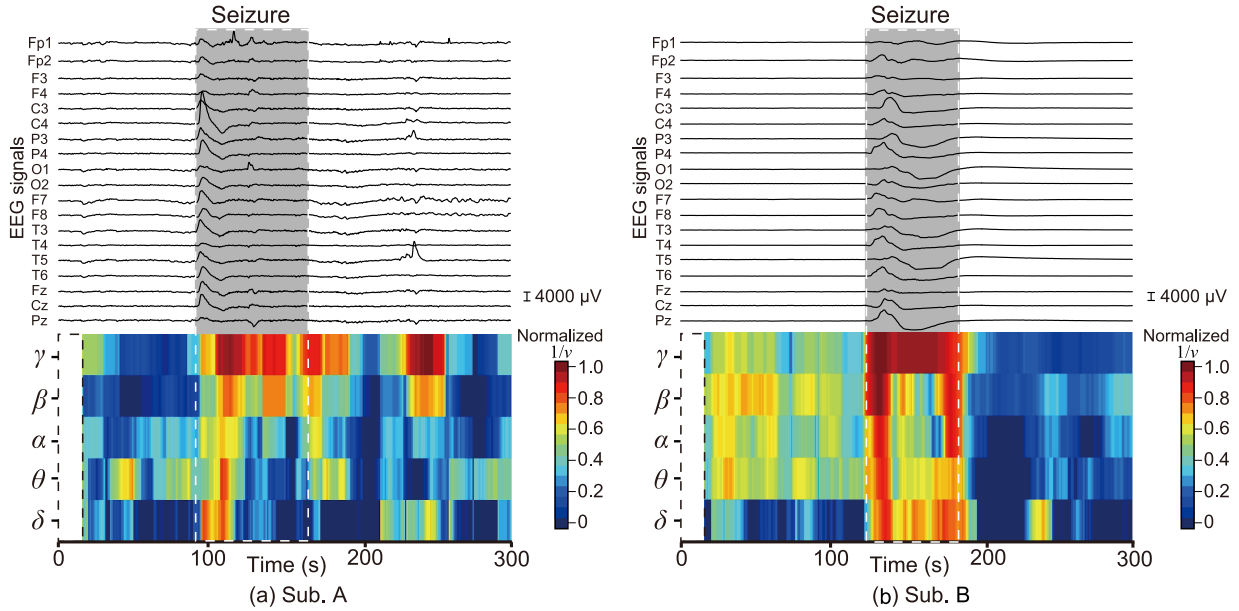

Fig. 6. Raw EEG signals and corresponding analysis results of the proposed method for (a) Sub. A and (b) Sub. B. Proposed index $1/\nu$ was normalized based on min–max normalization, rescaling the range of features to scale the range in [0, 1].

ガウスモデルの BIC が最小となる割合が 17.92%であり，他の帯域より多くなることが確認された．これは，低周波帯域では，それぞれの窓幅内の分布形状が大きく異なってしまうことが原因であると考えられる．また，提案モデルのパラメータ数 ($k_t = 382$) がガウスモデル ($k_g = 381$) よりも 1 大きいことからわずかな差でガウスモデルがより適したモデルであると判定されたと考えられる．ただし，その他の周波数帯域では，BIC が最小となる回数が 95%以上であり，提案モデルが他モデルより脳波に適したモデルであることがわかる．これは，提案モデルのパラメータ ν を変更させることで，外れ値が少ないガウスモデルと裾の重い分布となるコーシーモデル双方に適応できるためであると考えられる．また，高周波帯域になるにつれて，提案モデルの BIC が最小となる割合が増加している．これは，周波数特性に応じて脳波の分布も変化しており，信号の変化が速い高周波帯域の分布が提案モデルによく適合したためであると考えられる．

Fig. 6 より，てんかん発作区間において特に高周波帯域の $1/\nu$ が大きくなっていることがわかる．この傾向は，全ての被験者に共通して確認することができた．このことから，提案法を用いることで，てんかん発作に伴う脳波の非ガウス性の変化を確率的変動として定量的に評価できていると考えられる．しかしながら，Fig. 6(a) の 220 s 付近を見ると，てんかん発作以外の区間においても部分的な $1/\nu$ の増加が認められた．これは，筋電位などの高周波帯域のアーティファクトにより確率的変動が大きくなったためであると考えられるため，専門医の知見に基づき，解析結果についてより詳細に検討していく必要がある．

Fig. 7 より，全被験者の各帯域における $1/\nu$ の分布を確認すると，非発作時の $1/\nu$ は帯域によらず 0.02–0.03 の領域に分布していることがわかる．一方，発作時の $1/\nu$ は非発作時よりも大きい値で分布しており，その傾向は高周波である γ 帯域で最も顕著に表れていることがわかる．これは平均値の差の程度を表す効果量 g の結果からも確認できる．γ 帯域において大きな効果量が得られたことから，高周波帯域における $1/\nu$ がてんかん発作時の特徴を最も反映していると考えられる．これは，てんかん発作に伴い脳波の高周波帯域が強い非ガウス性を示したことを意味している．てんかん発作時に脳波の高周波帯域である γ 帯域の活動が活発になることは従来研究においても報告されている [26]–[28]．その詳しいメカニズムはいまだ明らかにされていないものの，皮質と皮質下構造の間の複雑な相互作用に起因すると考えられている [26]．この相互作用の異常によってんかん発作時特有の断続的な振幅変化が生じ，結果として高周波帯域の非ガウス性が強調され $1/\nu$ が増加した可能性がある．

Fig. 8(b) より，各帯域における $1/\nu$ の AUC を確認したところ，高周波帯域である γ 帯域で 0.881 と中程度ながら高い値が得られており，γ 帯域の $1/\nu$ が最も分類性能が高いことがわかる．また，従来の特徴量である RMS と有意な差を確認したため，γ 帯域の $1/\nu$ は従来の特徴量以上の識別性能を有することが示された．振幅の絶対的な大きさである RMS や振幅の情報をもつと考えられる $\boldsymbol{\Psi}$ と，提案法から算出される $1/\nu$ は脳波活動の異なる側面を捉えていると考えられるため，今後はこれらを組み合わせることでより高い識別性能を獲得できる可能性がある．

VI. Conclusion

本稿では，尺度混合モデルを用いて多チャネル脳波のモデル化を行なった．提案モデルにおいて，頭皮表面の多チャネル電極から計測された脳波を多変量ガウス分布，そしてその分散共分散行列を逆ウィシャート分布に従う確率変数として扱うことで，てんかん発作に伴う脳波の確率的変動を評価可能であることを示した．解析法では，脳波をフィルタバンクを用いて複数の周波数帯域に分解し，提案モデルに基づく推定を行なうことで，各周波数帯域における確率的変動を特徴づける指標を導入した．

シミュレーション実験では，各パラメータの推定精度を評価し，推定精度はサンプルサイズと次元数に依存して変

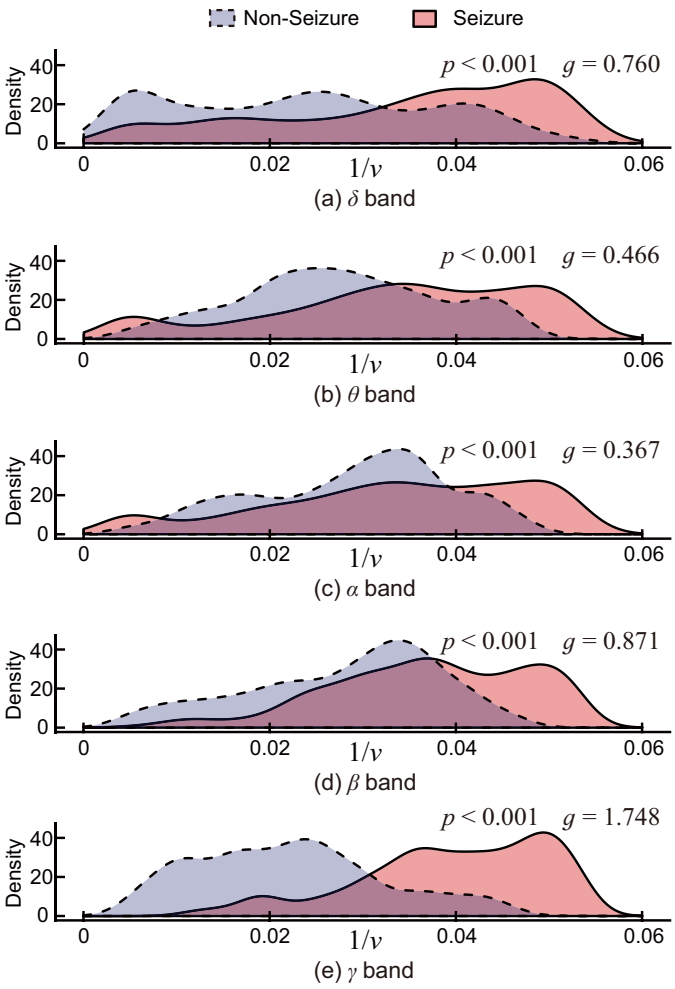

Fig. 7. Experimental distributions of $1/\nu$ estimated from EEG signals. The p value from paired t-test and the effect size g are also shown.

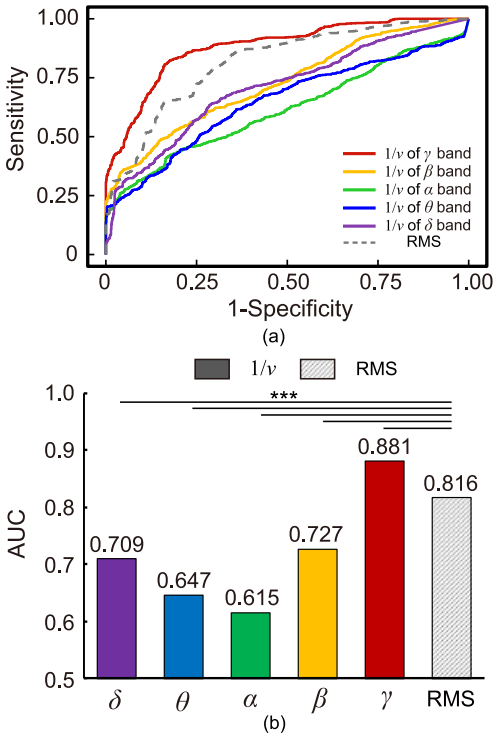

Fig. 8. Results of $1/\nu$ for each frequency band and RMS. (a) ROC curves. (b) AUCs. The pairwise comparisons between RMS and the others result based on the Delong's test for two correlated ROC curves with Holm adjustment are also shown (***: $p < 0.001$).

化することを示した．脳波解析実験においては，提案モデルが他モデルと比較して脳波に最も適したモデルであることを示し，γ 帯域の提案指標 $1/\nu$ に着目することで従来の特徴量よりも高い精度 (AUC=0.881) で分類可能であることを示唆した．

しかしながら，提案指標 $1/\nu$ は体動や体の硬直に起因する筋電図などのアーティファクトの影響を受けると考えられる．そのため，より実践的に提案法を展開するためには，これらのアーティファクトを検出・除去するようなアルゴリズムを導入する必要がある．また今後は，逆ウィシャート分布のもう一つのパラメータである $\mathbf{\Psi}$ の評価やてんかん脳波以外の脳波への応用を検討する予定である．

APPENDIX
EQUIVALENT CALCULATION ON MULTIVARIATE SMM

Equation (6) is equivalent to (9) as below:

$$
\begin{aligned}
p(\mathbf{x}_n) &= \int \mathrm{IG}(\tau_n; \nu'/2, \nu'/2)\mathcal{N}(\mathbf{x}_n|\tau_n\mathbf{\Psi}')\mathrm{d}\tau_n \\
&= \int \frac{\left(\frac{\nu'}{2}\right)^{\frac{\nu'}{2}}}{\Gamma\left(\frac{\nu'}{2}\right)}(\tau_n)^{-\frac{\nu'}{2}-1}\exp\left[-\frac{1}{\tau_n}\left(\frac{\nu'}{2}\right)\right] \\
&\quad \times \frac{1}{(2\pi)^{\frac{D}{2}}(\tau_n)^{\frac{D}{2}}|\mathbf{\Psi}'|^{\frac{1}{2}}}\exp\left[-\frac{1}{2}\mathbf{x}^{\mathrm{T}}(\tau_n\mathbf{\Psi}')^{-1}\mathbf{x}\right]\mathrm{d}\tau_n \\
&= \frac{1}{(2\pi)^{\frac{D}{2}}}\frac{\left(\frac{\nu'}{2}\right)^{\frac{\nu'}{2}}}{\Gamma\left(\frac{\nu'}{2}\right)}\frac{1}{|\mathbf{\Psi}'|^{\frac{1}{2}}} \\
&\quad \times \int (\tau_n)^{-\frac{\nu'+D}{2}-1}\exp\left[-\frac{1}{\tau_n}\left(\frac{\nu'+\Delta'}{2}\right)\right]\mathrm{d}\tau_n.
\end{aligned}
\tag{20}
$$

Multiply (20) of the equation by $\frac{\Gamma\left(\frac{\nu'+D}{2}\right)}{\left(\frac{\nu'+\Delta'}{2}\right)^{\frac{\nu'+D}{2}}} \times \frac{\left(\frac{\nu'+\Delta'}{2}\right)^{\frac{\nu'+D}{2}}}{\Gamma\left(\frac{\nu'+D}{2}\right)}$.

$$
\begin{aligned}
p(\mathbf{x}_n) &= \frac{1}{(2\pi)^{\frac{D}{2}}} \frac{\left(\frac{\nu'}{2}\right)^{\frac{\nu'}{2}}}{\Gamma\left(\frac{\nu'}{2}\right)} \frac{1}{|\mathbf{\Psi}'|^{\frac{1}{2}}} \frac{\Gamma\left(\frac{\nu'+D}{2}\right)}{\left(\frac{\nu'+\Delta'}{2}\right)^{\frac{\nu'+D}{2}}} \\
&\quad \times \int \frac{\left(\frac{\nu'+\Delta'}{2}\right)^{\frac{\nu'+D}{2}}}{\Gamma\left(\frac{\nu'+D}{2}\right)} (\tau_n)^{-\frac{\nu'+D}{2}-1} \\
&\quad \times \exp\left[-\frac{1}{\tau_n}\left(\frac{\nu'+\Delta'}{2}\right)\right] \mathrm{d}\tau_n \\
&= \frac{1}{(2\pi)^{\frac{D}{2}}} \frac{\left(\frac{\nu'}{2}\right)^{\frac{\nu'}{2}}}{\Gamma\left(\frac{\nu'}{2}\right)} \frac{1}{|\mathbf{\Psi}'|^{\frac{1}{2}}} \frac{\Gamma\left(\frac{\nu'+D}{2}\right)}{\left(\frac{\nu'+\Delta'}{2}\right)^{\frac{\nu'+D}{2}}} \\
&\quad \times \int \mathrm{IG}(\tau_n; \frac{\nu'+D}{2}, \frac{\nu'+\Delta'}{2}) \mathrm{d}\tau_n, \qquad (21)
\end{aligned}
$$

where the integral of probability density function over the entire space is equal to 1 (22).

$$
\int \mathrm{IG}(\tau_n; \frac{\nu'+D}{2}, \frac{\nu'+\Delta'}{2}) \mathrm{d}\tau_n = 1. \qquad (22)
$$

From (21) and (22), $p(\mathbf{x}_n)$ can be derived as follows:

$$
p(\mathbf{x}_n) = \frac{\Gamma(\frac{\nu'+D}{2})}{\Gamma(\frac{\nu'}{2})} \frac{|\mathbf{\Psi}'|^{-\frac{1}{2}}}{(\pi\nu')^{\frac{D}{2}}} \left(1 + \frac{\Delta'}{\nu'}\right)^{-\frac{\nu'+D}{2}}. \qquad (23)
$$

REFERENCES

[1] World Health Organization (WHO), "Epilepsy fact sheet," Accessed September 30, 2019.

[2] E. Kandel *et al.*, *Principles of neural science*. New York: McGraw-Hill, 2000, vol. 4.

[3] W. Deburchgraeve *et al.*, "Automated neonatal seizure detection mimicking a human observer reading EEG," *Clinical Neurophysiology*, vol. 119, no. 11, pp. 2447–2454, 2008.

[4] A. Subasi and E. Ercelebi, "Classification of EEG signals using neural network and logistic regression," *Computer methods and programs in biomedicine*, vol. 78, no. 2, pp. 87–99, 2005.

[5] P. Kellaway *et al.*, "Precise characterization and quantification of infantile spasms," *Annals of Neurology: Official Journal of the American Neurological Association and the Child Neurology Society*, vol. 6, no. 3, pp. 214–218, 1979.

[6] F. Panzica *et al.*, "Spectral properties of EEG fast activity ictal discharges associated with infantile spasms," *Clinical Neurophysiology*, vol. 110, no. 4, pp. 593–603, 1999.

[7] L. Fusco and F. Vigevano, "Ictal clinical electroencephalographic findings of spasms in West syndrome," *Epilepsia*, vol. 34, no. 4, pp. 671–678, 1993.

[8] N. Acir *et al.*, "Automatic detection of epileptiform events in EEG by a three-stage procedure based on artificial neural networks," *IEEE Transactions on Biomedical Engineering*, vol. 52, no. 1, pp. 30–40, 2005.

[9] B. R. Greene *et al.*, "A comparison of quantitative EEG features for neonatal seizure detection," *Clinical Neurophysiology*, vol. 119, no. 6, pp. 1248–1261, 2008.

[10] M. G. Sounders, "Amplitude probability density studies on alpha and alpha-like patterns," *Neurophysiology*, vol. 15, no. 5, pp. 761–767, 1963.

[11] F. F. Gonen and G. V. Tcheslavski, "Techniques to assess stationarity and gaussianity of EEG: An overview," *International Journal Bioautomation*, vol. 16, no. 2, pp. 135–142, 2012.

[12] G. V. L. J. Campbell, E. Bower, S. J. Dwyer, "On the Sufficiency of Autocorrelation Functions as EEG Descriptors," *IEEE Transactions on Biomedical Engineering*, vol. BME-14, no. 1, pp. 49–52, 1967.

[13] M. S. Weiss, "Non-Gaussian properties of the EEG during sleep," *Electroencephalography and Clinical Neurophysiology*, vol. 34, no. 2, pp. 200–202, 1973.

[14] M. Nurujjaman *et al.*, "Comparative study of nonlinear properties of EEG signals of normal persons and epileptic patients," *Nonlinear Biomedical Physics*, vol. 3, pp. 1–5, 2009.

[15] P. J. Charles *et al.*, "Non-Gaussian modeling of EEG data," *Proceeding 21st Conference Engineering in Medicine and Biology and the 1999 Annual Fall Meeting of the Biomedical Engineering Society. BMES/EMBS Conference*, no. 2, p. 1023, 1999.

[16] C. M. Bishop, *Pattern recognition and machine learning*. Springer New York, 2006.

[17] J. A. Bilmes, "A gentle tutorial of the EM algorithm and its application to parameter estimation for Gaussian mixture and hidden Markov models," *International Computer Science Institute*, vol. 4, no. 510, p. 126, 1998.

[18] C. F. V. L. Gene Howard Golub, *Matrix Computations*, 4th ed. The John Hopkins University Press, 2013.

[19] J. Hughes, *EEG in clinical practice*. Butterworth-Heinemann, 1994.

[20] G. Schwarz, "Estimating the dimension of a model," *The Annals of Statistics*, vol. 6, no. 2, pp. 461–464, 1978.

[21] M. Hamedi *et al.*, "Neural networkbased three-class motor imagery classification using time-domain features for BCI applications," *Region 10 Symposium 2014 IEEE*, no. Mi, pp. 204–207, 2014.

[22] E. Parzen, "On Estimation of a Probability Density Function and Mode," *The annals of mathematical statistics*, vol. 33, no. 3, pp. 1065–1076, 1962.

[23] L. V. Hedges, "Distribution Theory for Glass's Estimator of Effect Size and Related Estimators," *Journal of Educational Statistics*, vol. 6, no. 2, pp. 107–128, 1981.

[24] J. Cohen, *Statistical power analysis for the behavioral sciences*. Routledge, 2013.

[25] E. R. Delong and N. Carolina, "Comparing the Areas under Two or More Correlated Receiver Operating Characteristic Curves : A Nonparametric Approach," *Biometrics*, vol. 44, no. 3, pp. 837–845, 1988.

[26] K. Kobayashi *et al.*, "Very Fast Rhythmic Activity on Scalp EEG Associated with Epileptic Spasms," *Epilepsia*, vol. 45, no. 5, pp. 488–496, 2004.

[27] K. Kobayashi *et al.*, "Spectral analysis of EEG gamma rhythms associated with tonic seizures in Lennox-Gastaut syndrome," *Epilepsy Research*, vol. 86, no. 1, pp. 15–22, 2009.

[28] K. Benedek *et al.*, "Neocortical gamma oscillations in idiopathic generalized epilepsy," *Epilepsia*, vol. 57, no. 5, pp. 796–804, 2016.